First-Principles Full-Potential Calculations of the Fe *K* Pre-Edge and Near-Edge Structure in Carbonmonoxy-Myoglobin

M. Arfaoui[*], D. Cabaret[*], S. Della Longa[†,**], A. Seitsonen[*] and F. Mauri[*]

[*]*Institut de Minéralogie et de Physique des Milieux Condensés, CNRS UMR7590, Université Pierre et Marie Curie, Paris 6, 140 rue de Lourmel, F-75015 Paris, France*
[†]*Dipartimento Medicina Sperimentale, Università di L'Aquila, 67100 L'Aquila, Italy*
[**]*INFM, Università "LaSapienza", 00185Roma, Italy*

Abstract. The sensitivity of polarized Fe *K*-edge XANES spectra to Fe-C-O geometry is investigated in carbonmonoxy-myoglobin (MbCO) using first-principles non "muffin-tin" calculations. Structures issued from the Protein Data Bank (PDB) are optimized using Car-Parrinello dynamics and compared to experiment through simulations of X-ray absorption spectra. In order to understand the origin of the spectral features, trial structures are also considered. This paper shows that the combination of simulations of both pre-edge and near-edge regions allows a quantitative description of the iron environment in MbCO.

INTRODUCTION

Myoglobin (Mb) is a protein with similar biological functions and similar α side chain sequence to hemoglobin. Mb transports and stores oxygen in muscle tissues. Within the Mb structure, the polypeptidic chain constrains the heme ligation: it favours O_2 binding and discriminates against CO. This fact is directly correlated to the atomic details in the vicinity of Fe. Our purpose is to determine the geometry of the Fe-C-O bonds in MbCO.

Resolution lower than 1 Å in X-ray diffraction (XRD) experiments can lead to erroneous structural models around Fe. An alternative to XRD experiment is to combine experimental Fe *K*-edge X-ray absorption spectra with first-principles calculations. This paper presents a structural analysis by first-principles calculations of polarized X-ray absorption near-edge structure (XANES) spectra, recorded at the Fe *K*-edge in single crystals of MbCO and reported in Ref. [1]. First we focus on two structural models, listed in the PDB, that we optimize by Car-Parrinello molecular dynamics. Second we compute the XANES spectra from the experimental and optimized PDB models. Finally, we discuss the sensitivity of pre-edge and near-edge structures to the Fe-environment in terms of angles and distances.

METHODS

Calculations are performed starting from the 1A6G and 1BZR diffraction data of the PDB. These two structures are almost identical except in the vicinity of Fe (see Table 1). MbCO crystallizes in a monoclinic lattice (space group $P2_1$), with two molecules per unit cell. The crystal structures are optimized through Car-Parrinello molecular dynamics and simulated annealing using the CPMD code[1]. The framework is based on density functional theory (DFT) in the generalized gradient approximation (GGA) using BLYP exchange and correlation functional, plane-wave basis set (energy cut-off 100 Ry), norm-conserving (NC) pseudopotential, and periodic boundary conditions. The Brillouin zone (BZ) is sampled at the Γ point. Instead of the whole unit cell containing ~3000 atoms, we consider a 121 atom cluster including the heme molecule, the imidazole group linked to Fe (His93) and the two residues His64 and Val68 that constrain the C-O geometry. The cut bonds are protonated to ensure the cluster neutrality. The cluster is inserted in a cubic cell (18.5 $Å^3$) large enough to avoid interaction between clusters belonging to neighboring cells.

---

[1] "CMPD V3.9.1 Copyright IBM Corp 1999-2003, Copyright MPI fuer Festkoerperforschung Stuttgart 1997-2001".

TABLE 1. Description of the Fe environment: Comparison between XRD experimental data and first-principles energy minimization calculations.

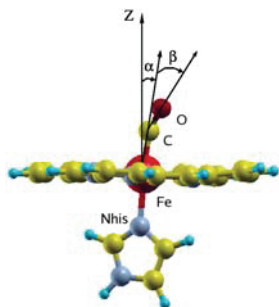| Models	Fe-Np (Å)	Fe-Nhis (Å)	Fe-C (Å)	C-O (Å)	$z_{Fe} - z_{heme\ plane}$ (Å)	α (°)	β (°)
1BZR exp.[2]	2.00	2.12	1.73	1.12	-0.015	4.8	7.4
1BZR relaxed	2.04-2.05	2.15	1.77	1.16	+0.05	8.6	6.9
1A6G exp.[3]	1.98	2.06	1.82	1.09	-0.001	9.0	9.0
1A6G relaxed	2.04	2.13	1.77	1.16	+0.05	8.6	8.6

FIGURE 1. Cluster used for XANES calculations.

XANES calculations are performed using similar plane-wave code[2], in which is implemented the calculation of X-ray absorption spectra [4, 5]. The spectra are calculated within DFT-GGA [6], using Troullier-Martins NC pseudopotentials, plane-wave basis set expanded to an energy cut-off of 70 Ry. We use a 48 atom cluster (Fig. 1). Using larger cluster does not provide significant changes in the theoretical spectra. The absorption cross section is computed as a continued fraction in both electric dipole (E_1) and quadrupole (E_2) approximations, using a broadening parameter γ constant in the first 5 eV (γ=1.36 eV) and linearly energy dependent above (slope 0.1). The self-consistent potential is determined on one k-point in the BZ, and the cross section computations require 4×4×4 k-point grids. The core-hole is taken into account by removing one $1s$ electron when generating the Fe pseudopotential.

RESULTS AND DISCUSSION

The results of the atomic relaxation are summarized in Table 1. The 1BZR and 1A6G relaxed structures are identical; only the angle β remains different.

Figures 2 and 3 compare experimental polarized spectra [1] with theoretical spectra for a polarisation parallel ($\sigma_\parallel$) and normal ($\sigma_\perp$) to the heme plane, respectively. The four calculated spectra correspond to the experimental and relaxed 1A6G and 1BZR models. For $\sigma_\parallel$,the four theoretical curves are almost identical. This result is expected since the structures are not much different in the heme plane. The agreement with

experiment is very good in the XANES region and less satisfactory in the pre-edge region, where peak p is located at too high energy. Some complementary calculations are in progress in order to understand the origin of this discrepancy, which could be related to the modeling of the core-hole interaction within DFT-
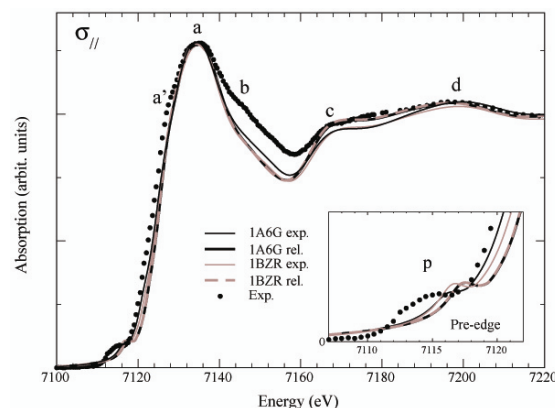

FIGURE 2. Experimental [1] and theoretical spectra for a polarisation in the heme plane ($\sigma_\parallel$).
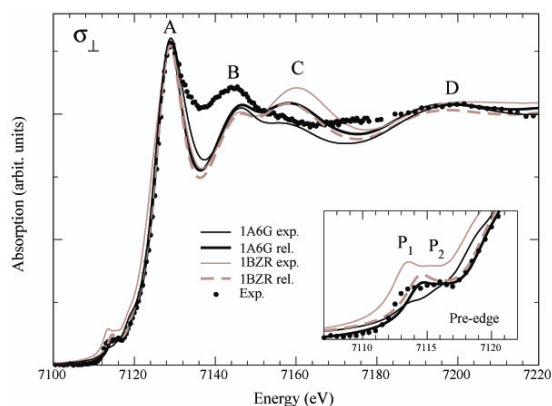

FIGURE 3. Experimental [1] and theoretical spectra for a polarisation normal to the heme plane ($\sigma_\perp$).

GGA. For $\sigma_\perp$, relaxed models lead to similar XANES calculated spectra that are in agreement with experiment especially in the pre-edge region. However, some discrepancies are noticeable. First, peak B is not satisfactorily reproduced in terms of intensity and energy position. The difference of intensities between peaks A and B is more pronounced in the calculated spectrum than in the experimental one, that is mainly due to a convolution problem. The energy position of peak B is at too high energy (~2

eV). We have found that the relative energy positions of peaks A and B are mainly correlated to the value of the β angle. Indeed we have made several calculations starting from the 1BZR relaxed model with β ranging
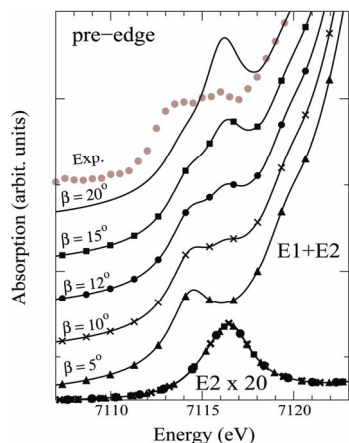

FIGURE 4. Effects of β angle on $\sigma_\perp$ theoretical pre-edge spectra. The E_2 contribution is multiplied by a factor 20.

from 0 to 30°. These simulations reveal that correct energy positions are obtained for an angle β =15 ± 5°, that is greater than experimental and theoretical values (see Table 1) but in good agreement with the result of the multiple scattering (MS) fitting procedure of Ref. [1]. Figure 4 shows that the investigation of the pre-edge region can allow the refinement of the β value. The E_2 transitions, which are displayed separately in Fg. 4, do not depend on β, and are very weak as compared to the E_1 ones. Varying the angle β modifies the hybridization between Fe d orbitals and CO antibonding π^* molecular orbitals. Figure 4 does show that pre-edge feature P_2 probes this hybridization via a $1s \rightarrow p$ transition, corroborating the interpretation given in [7]. The agreement with experiment is especially good for β ≈ 12°. The second main discrepancy between experiment and calculation in Fig. 3 concerns peak C that is too intense in the theoretical curves. It is even more intense with the 1BZR experimental model. The intensity of feature C appears to be correlated to the Fe-C distance and more generally to both the distances Fe-C and Fe-N$_{his}$. This is illustrated in Fig. 5, where in particular is displayed a calculated spectrum (black solid curve) obtained from the relaxed 1BZR model in which the Fe-C distance is increased to 1.83 Å (as in the 1A6G experimental model). Figure 5 shows that the intensity of peak C is inversely proportional to the Fe-C distance and that Fe-C should be greater than the optimized calculated one (i.e. 1.77 Å). Figure 3 also shows that the relative intensities of A, B, C and D peaks are better reproduced with the 1A6G experimental model, while in the pre-edge region the agreement is better with the relaxed models.
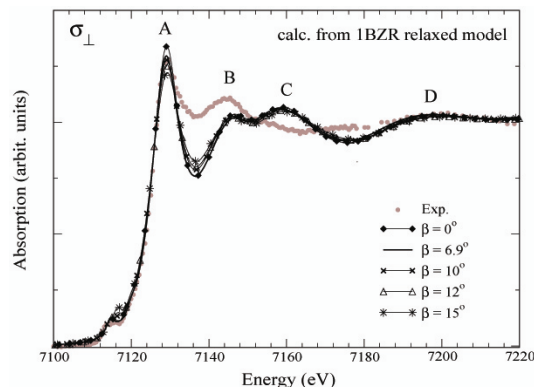

FIGURE 5. Effects of Fe-C and Fe-N$_{his}$ distances on $\sigma_\perp$.

CONCLUSION

Plane-wave pseudopotential codes are good tools to reproduce pre-edge and near-edge Fe K edge in hemoproteins. They permit the relaxation of the atomic positions by minimizing the total energy of the system. In MbCO the relaxation procedure underestimates the Fe-C distance. Self-consistent GGA+U calculations are in progress to understand this discrepancy. By combining calculations of both near-edge and pre-edge structure, it is possible to define the geometry of the Fe-C-O unit in terms of distances and angles. Peak C (intensity and energy position) is strongly affected by the Fe-C distance: Fe-C is found to be equal to ~1.82 Å, in agreement with the 1A6G experimental model and with MS fitting procedures of Ref. [1]. The pre-edge region can be more sensitive than the near-edge region to small details of the Fe environment: our calculations demonstrate that the strength of the second feature (P_2) of the pre-edge is controlled by angle β, that should be nearly equal to 12°. We acknowledge the computational support of the CNRS IDRIS center in Orsay, France (project 1202).

REFERENCES

1. S. Della Longa, A. Arcovito, M. Girasole, J. Hazemann, and M. Benfatto, *Phys. Rev. Lett.* **87**, 155501 (2001).
2. G. Kachalova, A. Popov, and H. Bartunik, *Science* **284**, 473–476 (1999).
3. J. Vojtechovsky, K. Chu, J. Berendzen, R. Sweet, and I. Schlichting, *Biophys. J.* **77**, 2153–2174 (1999).
4. M. Taillefumier, D. Cabaret, A.-M. Flank, and F. Mauri, *Phys. Rev. B* **66**, 195107 (2002).
5. D. Cabaret, E. Gaudry, M. Taillefumier, P. Sainctavit, and F. Mauri, *Physica Scripta* **T115**, 131–133 (2005).
6. J. P. Perdew, S. Burke, and M. Ernzerhof, *Phys. Rev. Lett.* **77**, 3865 (1996).
7. S. Della Longa, A.Arcovito, B. Vallone, A. C. Castellano, R. Khan, J. Vicat, Y. Soldo, and J. L. Hazemann, *J. Synchrotron Rad.* **6**, 1138–1147 (1999).